



# Catalytic conversion of glucose to methyl levulinate over metal-modified Beta zeolites

Atte Aho<sup>1</sup> · Narendra Kumar<sup>1</sup> · Kari Eränen<sup>1</sup> · Päivi Mäki-Arvela<sup>1</sup> ·  
Tappio Salmi<sup>1</sup> · Markus Peurla<sup>2</sup> · Ilari Angervo<sup>3</sup> · Jukka Hietala<sup>4</sup> ·  
Dmitry Yu. Murzin<sup>1</sup>

Received: 17 March 2022 / Accepted: 21 May 2022 / Published online: 9 June 2022  
© The Author(s) 2022

## Abstract

Methyl levulinate was selectively formed from glucose and methanol over a copper modified Beta zeolite bifunctional catalyst at 180 °C under argon atmosphere. The selectivity to methyl levulinate substantially exceeded previously reported in the open literature results. The copper modification was done through an ion-exchange method using a solution of copper nitrate, followed by drying and calcination of the catalyst. Copper modification changed the distribution of acid sites namely, less Brønsted and more Lewis sites were observed with FTIR using pyridine adsorption. Application of the proton form H-Beta-25 gave the methyl levulinate yield of ca. 89%, which could be elevated with the addition of copper, as the apparent selectivity exceeds 99%, assuming that methyl glucosides are eventually transformed to methyl levulinate. The non-acidic Cu/SiO<sub>2</sub> catalyst was completely inactive in methyl levulinate formation. Metal modification of Beta zeolite with Sn and Zn did not perform as well as Cu in the formation of methyl levulinate during glucose transformation.

**Keywords** Glucose · Methyl levulinate · Beta zeolite · Copper · Zinc · Tin

---

✉ Dmitry Yu. Murzin  
dmurzin@abo.fi

<sup>1</sup> Laboratory of Industrial Chemistry and Reaction Engineering, Johan Gadolin Process Chemistry Centre, Åbo Akademi University, Åbo, Finland

<sup>2</sup> Institute of Biomedicine, University of Turku, Turku, Finland

<sup>3</sup> Wihuri Physical Laboratory, University of Turku, Turku, Finland

<sup>4</sup> Neste Oyj, Porvoo, Finland

## Introduction

Levulinic acid is an important platform molecule [1] that can be used in several applications for the production of fuels, plasticisers, resins, polymers, herbicides, food flavourings and fragrances, anti-freeze agents and pharmaceuticals [2]. Levulinic acid can be produced through dehydration of glucose with 5-hydroxymethylfurfural (5-HMF) as an intermediate [3, 4] using mineral acids, such as hydrochloric and sulphuric acids [3, 5]. A drawback with the direct dehydration of glucose to levulinic acid is the high formation of humins [3, 6] that can decrease the yield of levulinic acid significantly. A way to overcome the humins formation is to perform the reaction in an alcohol giving levulinate esters instead [1, 7, 8]. A reaction scheme with the above discussed reactions are shown in Fig. 1.

Other drawbacks with the use of mineral acids are corrosion, dehydration of the alcohols forming ethers and a need of downstream neutralization of the acid [9]. A combination of both Brønsted and Lewis acids [10, 11] has been used for the conversion of cellulose to methyl levulinate. A catalytic system comprising of  $\text{In}(\text{OTf})_3$  and 2-naphthalenesulfonic acid gave a methyl levulinate yield of 75% at 180 °C. A semi-soluble aluminium salt ( $\text{Al}_2(\text{SO}_4)_3$ ) has been applied in the transformation of glucose and other sugars to methyl levulinate the highest report yield was 64% [12]. Heterogeneous catalysts can be used to overcome the drawbacks related to the mineral acids. In particular, solid acids, such as zeolites, can be applied in the transformation of glucose to either levulinic acid or methyl levulinate as reported in refs. [1, 9, 13].

Peng et al. [9] tested the catalytic performance of common zeolites namely, ZSM-5(25), ZSM-5(36) NaY, H-mordenite in the conversion of biomass carbohydrates to methyl levulinate at 200 °C. The main product after a 2 h experiment was, however, methyl glucoside when using zeolites as the catalysts. Peng et al. tested also other solid catalysts such as  $\text{Zr}_3(\text{PO}_4)_4$ ,  $\text{SO}_4^{2-}/\text{ZrO}_2$ ,  $\text{SO}_4^{2-}/\text{TiO}_2$  and  $\text{TiO}_2$ . The most promising catalyst was sulphated titania giving a methyl levulinate yield of 33% when using glucose as the reactant, while slightly better yields were obtained with fructose (43%) and sucrose (59%). A possible reason for a higher methyl levulinate yield starting from fructose could be due to the reaction network for methyl levulinate formation from glucose with isomerization to fructose as the initial step [14]. Clay materials, namely metal modified montmorillonite, have also been applied in the conversion of glucose to methyl levulinate [14]. A significantly higher methyl levulinate yield (60.7%) could be obtained with an  $\text{Al}^{3+}$  ion-exchanged montmorillonite catalyst [10] compared to the values reported by Peng et al. [9]. Copper modified montmorillonite gave also a relatively high methyl levulinate yield (58.7%) [14].

This work will report the outstanding performance of copper modified Beta zeolites as well as results for other catalysts, including zinc and tin modified beta, proton form beta and copper on silica for the transformation of glucose to methyl levulinate significantly exceeding the results reported in the literature. A further important aim of the current investigation was to study the influence of the

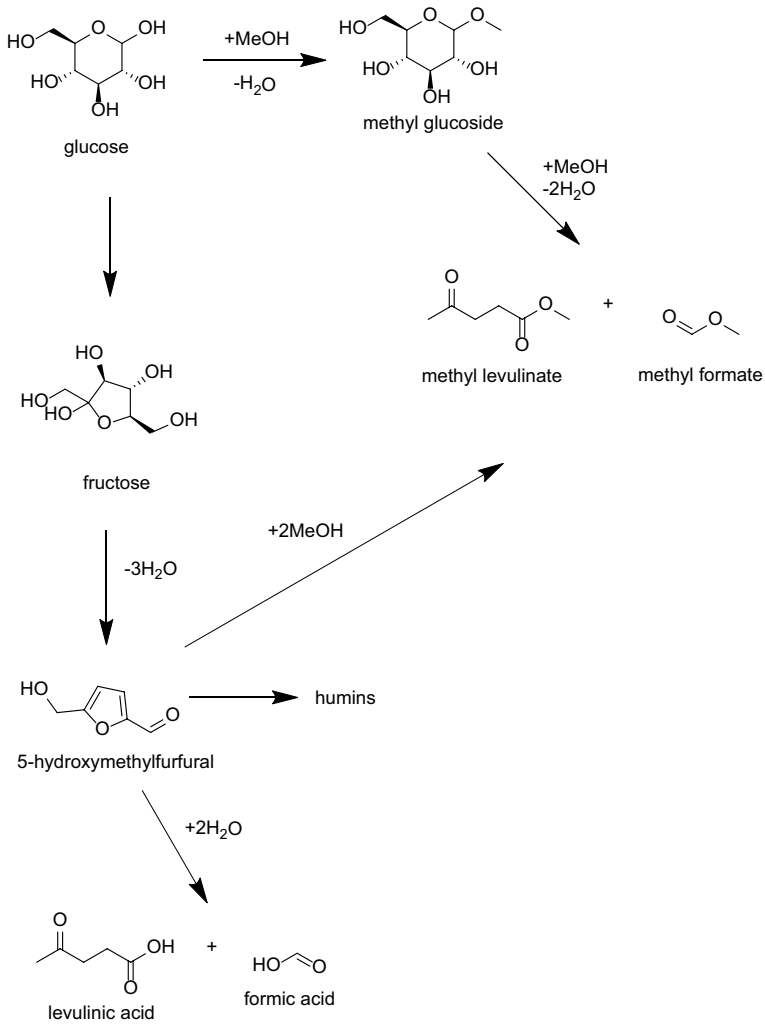


**Fig. 1** Reaction scheme for glucose transformation to levulinic acid and methyl levulinate

methods of metal (Cu, Zn, Sn) modifications such as ion-exchange and evaporation impregnation on the physico-chemical and catalytic properties of Beta zeolite catalysts.

## Experimental

### Catalyst preparation

#### Cu-modification

Synthesis of the Cu-modified catalysts was carried out by the ion-exchange method using aqueous solutions of copper nitrate to afford a better metal dispersion. 2.56 g of copper nitrate trihydrate (> 99%, Fluka) was dissolved in 500 mL of distilled water followed by adding 10 g of H-Beta-25 (Zeolyst International, CP814E) or H-Beta-300 (Zeolyst International, CP811C-300). The numbers (25 and 300) after the zeolite name correspond to the  $\text{SiO}_2/\text{Al}_2\text{O}_3$  molar ratio. After the synthesis performed using continuous stirring for 24 h, the catalyst was filtered and washed with distilled water. Drying of the catalyst was carried out in an oven at 100 °C followed by calcination at 400 °C in a muffle oven using a step calcination procedure.

#### Sn-modification

Sn-H-Beta-38 catalyst was synthesized using an evaporation impregnation method. 3.58 g  $\text{SnCl}_2 \cdot 2\text{H}_2\text{O}$  was dissolved in 250 mL of distilled water in a flask. The synthesis of Sn-H-Beta-38 (Zeolyst International, CP814C\*) catalyst was carried out in Büchi Rotavapor evaporator for 24 h. Another Sn-modified (de-Al-Sn-H-Beta-38) catalyst was prepared with the same procedure but with a dealuminated H-Beta-38 zeolite. The dealumination was performed with 1 M  $\text{HNO}_3$  treatment. A third Sn-modified Beta zeolite (Sn-H-Beta-300) was also prepared using an ion-exchange method. 3.58 g of  $\text{SnCl}_2 \cdot 2\text{H}_2\text{O}$  precursor was dissolved in 500 ml distilled water. 10 g of H-Beta-300 (Zeolyst International, CP811C-300) was added to  $\text{SnCl}_2$  aqueous solution with stirring. The synthesis was performed with continuous stirring for 24 h. After completion of synthesis, the catalytic material was filtered and washed with 2000 mL of distilled water.

After completion of synthesis, the catalysts were dried at 100 °C in an oven for 7 h. The thermal treatment of the catalyst was carried out in a muffle oven at 400 °C using the step calcination procedure.

#### Zn-modification

Evaporation impregnation method was utilized to modify H-Beta-25 zeolite (Zeolyst International, CP814E) with zinc. A 250 mL solution containing 3.56 g of  $\text{Zn}(\text{NO}_3)_2 \cdot 6\text{H}_2\text{O}$  was prepared, 5 g of the zeolite was added to the solution. The impregnation was carried out at 60 °C for 24 h prior evaporation of the liquid. The catalyst was calcined at 425 °C for 3 h.

## Catalyst characterization

The prepared metal modified catalysts were characterized with different techniques. The concentration of Brønsted and Lewis acid sites was measured using FTIR and pyridine as the probe molecule. Both scanning and transmission electron microscopy were used to elucidate morphology and the textural properties. The specific surface area and the pore size distributions were determined by nitrogen physisorption. The phase purity of the catalysts was confirmed by XRD. More details are provided below.

A FTIR (ATI Mattson Infinity Series) was used for determining the strength and concentrations of both Brønsted and Lewis acid sites. The metal modified Beta zeolites were pressed into thin wafers and placed into the FTIR cell, which was outgassed and heated to 450 °C for 1 h. Thereafter the cell was cooled to 100 °C and the background spectra was recorded. Pyridine (> 99%, Acros Organics) was adsorbed to the catalytic acid sites during 30 min followed by desorption at 250 °C, 350 °C and 450 °C under vacuum for 1 h at each temperature. Spectral bands at 1545  $\text{cm}^{-1}$  and at 1450  $\text{cm}^{-1}$  were used to identify Brønsted (BAS) and Lewis (LAS) acid sites. The concentrations of acid sites were calculated using the extinction coefficients reported by Emeis [15].

The crystal morphology, shape and size of the catalysts were studied with scanning electron microscopy (SEM) using a (Leo Gemini 1530) microscope. The elemental compositions of the catalysts were analyzed by energy-dispersive X-ray spectroscopy (EDX) coupled to the SEM. The presence of metal nanoparticles and porosity of the catalysts were investigated by transmission electron microscopy (TEM) using a (JEOL JEM-1400 Plus) microscopy equipped with a bottom mounted (OSIS Quemesa) digital camera.

The specific surface area, pore size and the pore volume of the catalysts were measured with a (Micrometrics MicroActive 3Flex3500). Prior to the surface area measurements, the catalyst samples were outgassed at 250 °C for 4 h. The specific surface was calculated with the Dubinin-Radushkevich method and the pore size and volume with the Horvath-Kawazoe method.

The X-ray diffraction (XRD) characterization was performed using a (PANalytical Empyrean) diffractometer. The results were obtained with a  $2\theta$  scan range from 5° to 120°.

## Glucose conversion experiments

Transformations of glucose over the metal modified Beta zeolites were carried out in a batch reactor equipped with a gas entrainment impeller, a heating mantle and a sampling line. The gas atmosphere in the set-up was argon (Linde, 5.0), as the intention was to use an inert gas preventing any contact with oxygen.

The glucose conversion experiments were carried out by loading the reactor vessel with 0.41 g of the catalyst (< 63  $\mu\text{m}$ ), 0.9 g glucose (> 98%, Fluka) and 100 mL methanol (> 99.9%, Sigma-Aldrich). Experiments with higher glucose concentrations were not pursued because of a limited solubility of glucose in methanol. After

the reactor was filled with the reactants and the catalyst, it was flushed with argon. Thereafter, heating to 180 °C was started with a 3 °C/min heating rate. When the reactor temperature reached 180 °C the sampling ( $t=0$  min) and stirring (720 rpm) were started. The samples were withdrawn from the reactor through a 7  $\mu\text{m}$  sinter to avoid removal of catalyst particles, moreover, prior to analysis the liquid sample was further filtered through a 0.43  $\mu\text{m}$  syringe filter. The samples were initially analysed by HPLC, and by GC after achieving practically full sugar conversions. A selection of the liquid samples was also analysed by NMR.

## Product analysis

The composition of the reaction mixture was analysed by high performance liquid chromatography (HPLC). The HPLC (Hewlett Packard 1100 series) was equipped with a refractive index detector (RI), the column used for separation of the compounds operating at 45 °C was an (Animex HPX-87H) applying 5 mM sulphuric acid as the eluent with the flow rate 0.6 mL/min. The response factors as well as the retention times for several different compounds (glucose, fructose,  $\alpha$ - and  $\beta$ -methyl glucoside) were determined prior to catalytic experiments and used for calculations of the concentrations. The presence of  $\alpha$ - and  $\beta$ -methyl glucoside was verified by NMR.

The NMR spectra were measured on an (AVANCE III spectrometer Bruker Biospin GmbH, Rheinstetten, Germany) operating at 500.20 MHz for  $^1\text{H}$ , equipped with a 1H/BB SmartProbe. The  $^1\text{H}$  spectrum was recorded in MeOD- $d_4$ .

After most of the sugars had been converted, based on HPLC analysis, the samples were analysed by GC (HP 6890) equipped with an HP-5, 5% Phenyl Methyl Siloxane 30.0 m  $\times$  320  $\mu\text{m}$   $\times$  0.50  $\mu\text{m}$  nominal, column. The eluting components were detected by the flame ionisation detector (FID). The temperature program used in the analysis was as follows: 2 min at 40 °C, heating with 10 °C/min to 250 °C and holding for 3 min. The gas flow through the column was set to 3.8 mL/min. The response factors as well as retention times for several different compounds were determined and used for calculations of the concentrations. The calibrated compounds were: methyl lactate, methyl formate, methyl levulinate and furfural.

## Results and discussion

### Glucose transformations

The sugar concentrations during the glucose transformations over Cu-H-Beta-25 are displayed in Fig. 2.

The presence of methyl glucosides was verified by NMR for the sample taken at 60 min where the concentration of  $\alpha$ -methyl glucoside was the highest. The NMR spectrum is presented in Fig. 3. The previously reported results [9] correspond well to our findings namely that methyl glucosides are formed at the beginning of glucose transformations to methyl levulinate. Peng et al. [9] carried out their experiments for

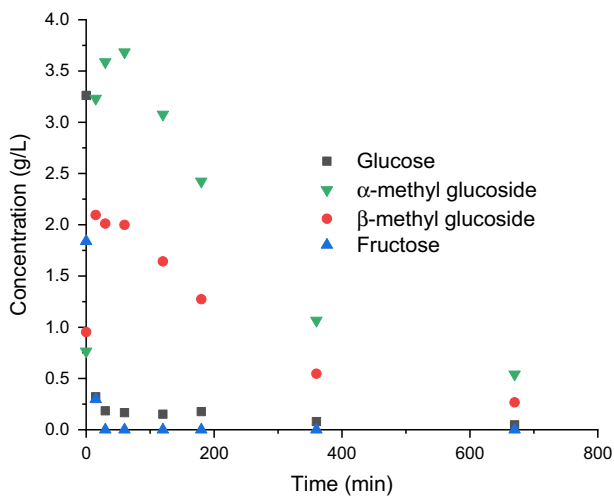


**Fig. 2** Concentration of the reactants and some products during glucose transformations over Cu-H-Beta-25 catalyst at 180 °C

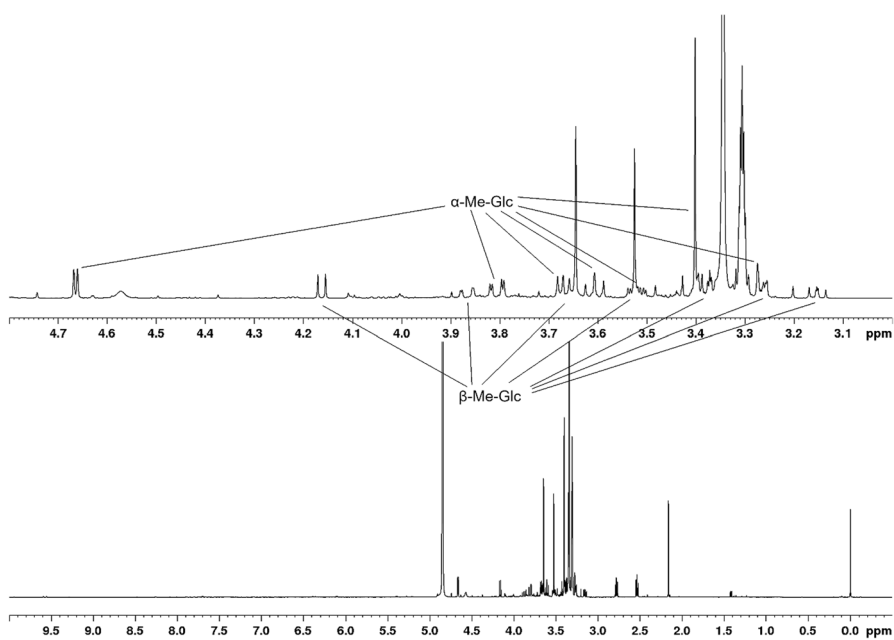


**Fig. 3** NMR spectrum for the 60 min sample showing signals for α- and β-methyl glucosides. Glucose transformations were carried out at 180 °C over Cu-H-Beta-25 catalyst

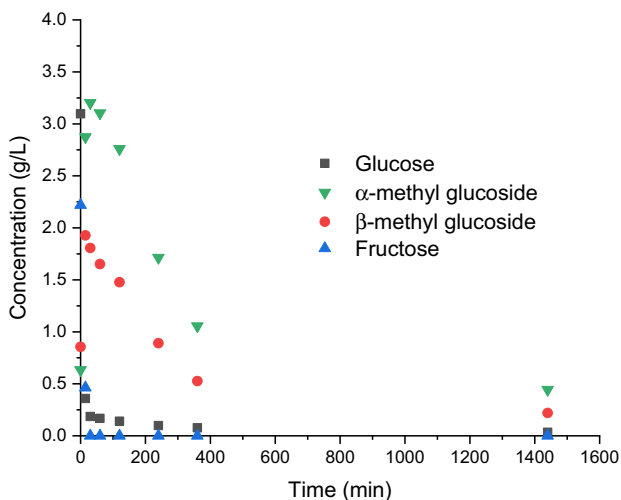
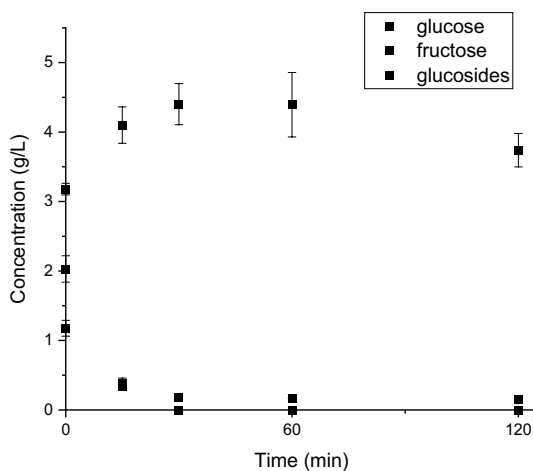


**Fig. 4** Concentration profiles for the reactants and some products during a 24 h experiment at 180 °C over Cu-H-Beta-25

**Fig. 5** The average concentrations of glucose, fructose and methyl glucosides obtained in glucose transformation over Cu-H-Beta-25 as a function of time



2 h only, however, at a higher temperature (i.e. 200 °C) and reported methyl glucosides as the main products with different zeolites as catalysts.

From Fig. 2, it can be observed that the concentrations of the methyl glucosides did not decrease to zero after 11 h, therefore, the reaction duration should be prolonged to achieve higher conversions. The concentration profiles for a 24 h run are shown in Fig. 4.

The average concentrations for glucose and the products and the experimental errors of the results depicted in Figs. 2 and 4 were also plotted as a function of time up to 120 min (Fig. 5) showing that the maximum error in glucose and fructose



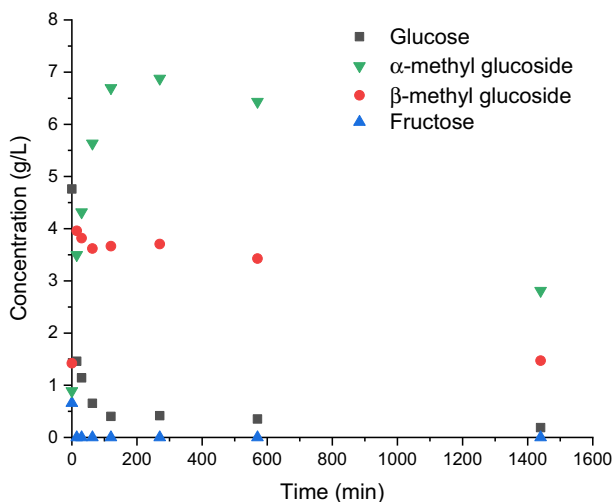


**Fig. 6** Concentration profiles of the reactants and products during a 24 h experiment at 180 °C over Cu-H-Beta-300

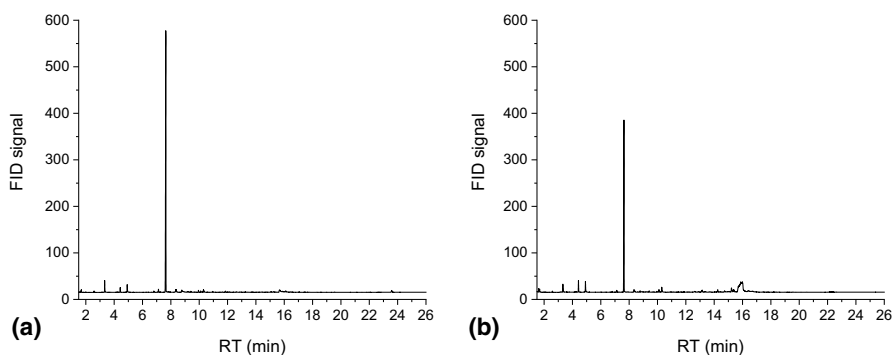


**Fig. 7** GC chromatograms for the final (24 h) samples with different copper modified catalysts, **a** Cu-H-Beta-25, **b** Cu-H-Beta-300. A large peak of methanol at RT 1 min is not shown

concentrations were 2.5% and 9%, respectively, while for glucosides it was 10%. These results demonstrate a sufficient accuracy of the experimental results.

A similar experiment was also carried out over Cu-H-Beta-300. The sugar concentration profiles are demonstrated in Fig. 6.

Comparing these sugar concentration profiles displayed in Figs. 4 and 6 it can be observed that conversion of  $\alpha$ - and  $\beta$ -methyl glucosides is considerably slower over Cu-H-Beta-300 compared to Cu-H-Beta-25. A possible reason for the differences can be attributed to differences in the acid site concentrations and acid strength, as discussed below.

The final (24 h) samples displayed in Figs. 4 and 6 were further analysed by GC, with the chromatograms presented in Fig. 7.

As seen in Fig. 7, essentially one major peak visible in both cases originates from methyl levulinate. Based on the response factor the concentrations of methyl levulinate over the Cu-H-Beta-25 is 6.03 g/L while the corresponding value for Cu-H-Beta-300 is 3.66 g/L. These concentrations correspond to the methyl levulinate yields of ca. 93% and 56% for Cu-H-Beta-25 and Cu-H-Beta-300 catalysts, respectively. The results for all tested catalysts are compiled in Table 1.

The methyl levulinate yield was calculated by dividing the concentration of methyl levulinate with the initial concentration of glucose. The sugar conversion was calculated by dividing the difference between the initial glucose concentration and the concentrations of glucose, fructose,  $\alpha$ - and  $\beta$ -methyl glucosides with the initial glucose concentration. From Table 1 high conversion can be observed for most of the catalysts for the final samples apart from Cu-H-Beta-300 and Sn-H-Beta-300 when lower levels of sugar conversion were obtained, while glucose conversion over all catalysts was very high.

For comparison, experiments with the proton form of H-Beta-25 zeolite as well as copper on silica, Cu/SiO<sub>2</sub>, were tested. The methyl levulinate yield over H-Beta-25 was 89.2% at full sugar conversion while over Cu/SiO<sub>2</sub> no methyl levulinate was detected. In essence, the results demonstrated the superior performance of the bi-functional copper beta zeolites, while the experiments with the non-acidic Cu/SiO<sub>2</sub> catalyst gave no levulinate. The proton form H-Beta-25 exhibited a fairly good methyl levulinate yield, thus by combining both copper and the acidic zeolite, as used in this work, the potential methyl levulinate selectivity (comprising also methyl glucosides) can be increased to nearly 100%. Modification of the zeolite with tin or zinc had a negative effect in the methyl levulinate yield even at high conversions, as follows from Table 1. As shown in the reaction scheme in Fig. 1, methyl formate is formed in 1:1 ratio with methyl levulinate. However, because methyl formate has a very low boiling point (32 °C) a major part of this compound is evaporated during sampling and is therefore not detected by GC. Another reason for not detecting methyl formate could be that it decomposes to either CO or CO<sub>2</sub>.

In the literature glucose conversion to methyl levulinate over Sn-Al- $\beta$  zeolite has been reported previously [16]. The authors [16] stated that modification of Beta zeolite with tin using incipient wetness impregnation of SnCl<sub>4</sub> increased Lewis acidity of the zeolite. A higher Lewis acidity was linked with easier isomerization of glucose to fructose, which is one of the initial steps in glucose transformation to methyl levulinate. Yang et al. [16] used also the hydrothermal treatment of Sn-Al-Beta zeolite with tetraethylammonium hydroxide to increase mesoporosity. Both introduction of tin, resulting in a higher Lewis acidity, and the hydrothermal treatment, resulted in an improved catalyst performance for methyl levulinate formation. The improvement compared to the parent zeolite was 2.3 fold, corresponding to the methyl levulinate yield of 49% [16]. Clearly the results reported here can be considered superior compared to previously reported [16] methyl levulinate yields.

Commercially available H-Beta-25, a one similar to the zeolite used in this work, has been tested in the synthesis of methyl levulinate from 5-hydroxymethylfurfural [6]. The experiments were carried out at different temperatures ranging from 50 to 170 °C and under oxygen atmosphere (0–20 bars). Other zeolites besides H-Beta-25 were also tested namely, H-Beta-40, ZSM-5 (27, 50 and 130) as well

**Table 1** Catalytic results with different catalyst, concentrations of glucose, fructose,  $\alpha$ - and  $\beta$ -methyl glucosides as well as methyl levulinate in mmol/L, glucose and sugar conversion, yield of methyl levulinate and TOF for formation of methyl levulinate at the end of the reaction calculated as formed amount of methyl levulinate per the amount of Brønsted acid sites (Table 2), and time

Entry	Catalyst	Time (min)	Glucose	Fructose	$\alpha$ -methyl glucoside	$\beta$ -methyl glucoside	methyl levulinate	$X_{\text{glu}}$ (%)	$X_{\text{S}}$ (%)	Y (%)	TOF ( $\text{h}^{-1}$ )
1	Cu-H-Beta-25	1440	0.17	0.00	2.27	1.13	46.33	100	92.9	92.8	32.2
2	Cu-H-Beta-300	1440	1.05	0.00	14.47	7.57	28.12	98	53.8	56.3	75.2
3	H-Beta-25	1440	0.00	0.00	0.10	0.05	44.57	100	99.7	89.2	15.4
4	Cu/SiO <sub>2</sub>	1440	0.33	2.72	0.62	0.46	0.00	99	91.7	0.0	n.a
5	Zn-H-Beta-25	1455	0.00	0.00	1.29	0.46	9.07	100	96.5	18.2	n.a
6	Sn-H-Beta-38	360	0.11	0.00	1.70	0.82	17.06	100	94.7	34.1	35.4
7	Sn-H-Beta-300	360	0.89	0.00	18.90	9.94	15.14	98	40.5	30.3	108.0
8	de-Al-Sn-H-Beta-38	360	0.11	0.00	1.85	0.88	26.05	100	94.3	52.1	87.5

as USY-5.4 [6]. It was reported that the humin formation could be diminished at reaction temperatures higher than 150 °C and the oxygen pressure above 10 bar [6]. The highest methyl levulinate yield reported by Wang et al. [6] was 69.6% from 5-hydroxymethylfurfural. Our results showing methyl glucosides as intermediates gave a significantly higher yield of methyl levulinate compared to Ref. [6], indicating that humin formation from methyl glucosides occurs to a lesser extent than in the case of 5-hydroxymethylfurfural as a substrate over similar catalysts.

TOF for formation of methyl levulinate was also calculated per amount of Brønsted acid sites (Table 1) at the end of the reaction. The comparison of the TOF values for the long duration experiments over Cu-H-Beta-25, Cu-H-Beta-300 and H-Beta-25 (Table 1, entries 1–3) illustrates that the highest TOF was observed for Cu-H-Beta-300 exhibiting the lowest concentration of Brønsted acid sites. Thereafter, the TOF declined with an increasing amount of the Brønsted acid sites giving the second highest TOF for Cu-H-Beta-25 and the lowest for H-Beta-25. This result is somewhat contradicting to the data reported in the literature [16], where, however, the values correspond to 30 min reaction time reflecting thus the initial TOF. In the current case the TOF values averaged for the whole duration of experiments are given, because sugars present in the reaction mixture prevented direct GC analysis of methyl levulinate. It should be, on the other hand mentioned, that an analogous trend of decreasing TOF values with an increasing amount of Brønsted acid sites was also observed for experiments of a shorter duration (Table 1, entries 6–8).

## Catalyst characterization results

Acidity of the prepared catalysts was determined by FTIR using pyridine as a probe molecule. The FTIR spectra for Cu-H-Beta-25 catalyst after desorption at 250 °C, 350 °C and 450 °C are given in Fig. 8, showing pyridine adsorbed on Brønsted (1450  $\text{cm}^{-1}$ ) and Lewis (1550  $\text{cm}^{-1}$ ) acid sites.

The measured concentrations of acid sites used in this work are listed in Table 2.

**Table 2** Concentration of Brønsted and Lewis acid sites for the different Beta zeolite catalysts

Catalyst	Brønsted acid sites ( $\mu\text{mol/g}$ )			Lewis acid sites ( $\mu\text{mol/g}$ )		
	250 °C	350 °C	450 °C	250 °C	350 °C	450 °C
H-Beta-25	294	226	146	66	25	6
H-Beta-38	278	261	221	31	12	2
Cu-H-Beta-25	146	192	93	152	32	4
Cu-H-Beta-25-REG	184	184	143	132	47	3
Cu-H-Beta-300	38	38	2	45	15	3
Sn-H-Beta-38	196	188	43	50	11	0
de-Al-Sn-H-Beta-38	121	101	53	65	17	2
Sn-H-Beta-300	57	55	27	76	26	7
Zn-H-Beta-25	41	22	13	234	154	109

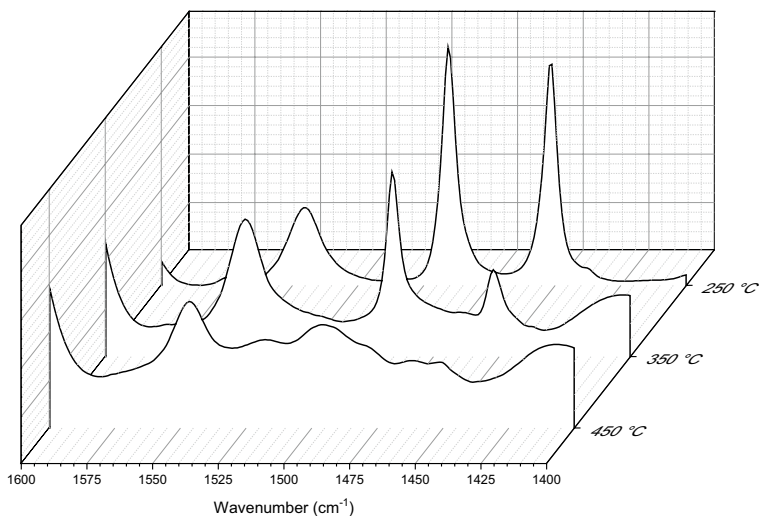


**Fig. 8** FTIR spectra of pyridine adsorbed on Cu-H-Beta-25 after desorption at 250 °C, 350 °C and 450 °C

Table 2 clearly illustrates that the distribution of acid sites is changed after metal modification for different Beta zeolites. In particular the total amount of Brønsted sites decreased approximately by half and the total amount of Lewis sites increased more than twofold for Cu-modified catalysts. The change in acid site distribution was even higher for the Zn-modified Beta-25 zeolite, where the total amount of Brønsted site decreased to ca. 1/7 and the content of Lewis sites increased by a factor of ca. 4. Acidity of Cu-H-Beta-25-REG was measured after regeneration at 400 °C in air. The total number of acid sites of the regenerated catalyst is higher for Brønsted and lower for Lewis sites. Not surprisingly, Brønsted acidity of Cu-H-Beta-25 and Sn-H-Beta-38 is significantly higher than for Cu-H-Beta-300 and Sn-H-Beta-300.

The catalysts were visualized by both scanning (SEM) and transmission (TEM) electron microscopies. SEM images for Cu-H-Beta-25 are presented in Fig. 5, showing typical morphologies for Beta zeolite. The copper content in Cu-H-Beta-25 analysed by energy-dispersive X-ray spectroscopy (EDX) was 0.85 wt%, while the corresponding values for Sn-H-Beta-38, Sn-H-Beta-300 and Zn-H-Beta-25 were 7.71, 7.78 and 9.7 wt%. Worth mentioning is that presence of Cl was not observed in Sn containing catalyst prepared with tin chloride as a precursor.

TEM images for the same catalyst shown in Fig. 9, did not display any copper nanoparticles indicating that copper was indeed ion-exchanged with the acid sites of the Beta zeolite, most likely the Brønsted sites, and thus has a very high dispersion (Fig. 10).

The specific surface area, pore size and volume for the fresh and regenerated Cu-H-Beta-25 catalysts are listed in Table 3.

The nitrogen physisorption results listed in Table 3 are comparable for both the fresh and regenerated catalysts, having similar specific surface areas as well as

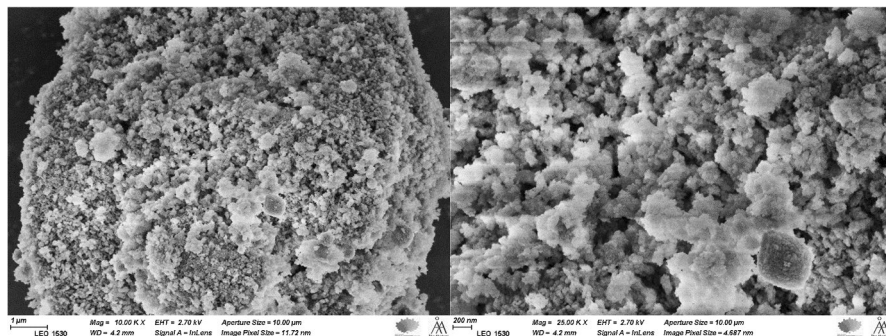


Fig. 9 SEM images of Cu-H-Beta-25 catalyst

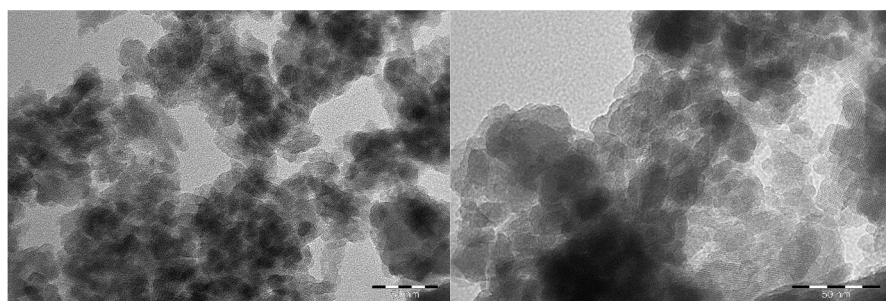


Fig. 10 TEM images of the Cu-H-Beta-25 catalyst

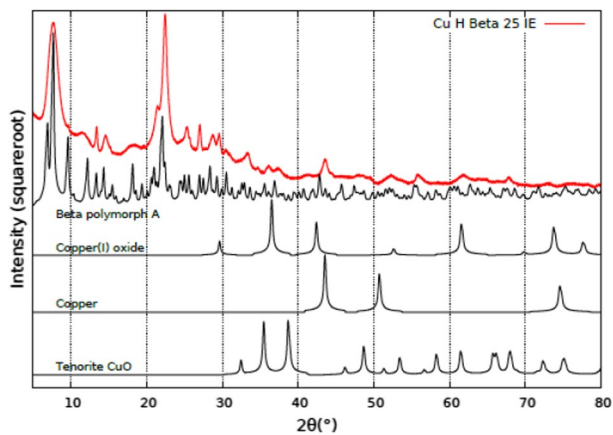


Fig. 11 XRD for Cu-H-Beta-25 with the standardized diffraction patterns for Beta polymorph A, CuO, Cu and Cu<sub>2</sub>O

**Table 3** Specific surface area, pore size and volume for fresh and regenerated Cu-H-Beta-25 catalysts

Catalyst	Specific surface area (m <sup>2</sup> /g)	Median pore size (nm)	Pore volume (mL/g)
Cu-H-Beta-25	492	0.69	0.18
Cu-H-Beta-25-REG	473	0.69	0.17

pore sizes and volumes, illustrating that there was almost no carbon deposits after regeneration.

The X-ray diffraction results for Cu-H-Beta-25 are presented with calculated diffraction patterns for Beta polymorph A [17], CuO [18], Cu [19] and Cu<sub>2</sub>O [20] in Fig. 11. It is clear that the main features can be explained with Beta polymorph A phase, although the standard diffraction patterns for Cu and its oxides match with some of the diffraction details, preventing unequivocal identification.

## Conclusions

Metal modified Beta zeolite catalysts were prepared, characterized and tested in glucose transformation at 180 °C in methanol. Copper modification of the Beta zeolite changed the distribution of acid sites, namely the amount of Brønsted sites decreased while the number of Lewis sites increased. XRD analysis of Cu-H-Beta-25 catalyst showed that the main features of the XRD-pattern corresponds to Beta polymorph A. Cu-H-Beta-25 catalyst was very selective to methyl levulinate, giving after 24 h the yield of methyl levulinate of 92.6% at complete conversion of the reactant.

**Acknowledgements** This work is part of the activities of the Johan Gadolin Process Chemistry Centre at Åbo Akademi University. The authors are grateful to Dr. Jani Rahkila from the Instrument Centre at Åbo Akademi for performing the NMR analysis. Electron microscopy samples were processed and analyzed in the Electron Microscopy Laboratory, Institute of Biomedicine, University of Turku, which receives financial support from Biocenter Finland.

**Funding** Open access funding provided by Abo Akademi University (ABO).

## Declarations

**Competing interests** The authors declare no competing interests.

**Open Access** This article is licensed under a Creative Commons Attribution 4.0 International License, which permits use, sharing, adaptation, distribution and reproduction in any medium or format, as long as you give appropriate credit to the original author(s) and the source, provide a link to the Creative Commons licence, and indicate if changes were made. The images or other third party material in this article are included in the article's Creative Commons licence, unless indicated otherwise in a credit line to the material. If material is not included in the article's Creative Commons licence and your intended use is not permitted by statutory regulation or exceeds the permitted use, you will need to obtain permission directly from the copyright holder. To view a copy of this licence, visit <http://creativecommons.org/licenses/by/4.0/>.

## References

1. Hu X, Li CZ (2011) Levulinic esters from the acid-catalysed reactions of sugars and alcohols as part of a bio-refinery. *Green Chem* 13:1676–1679
2. Hayes GC, Beyer R (2020) Levulinic acid: a sustainable platform chemical for novel polymer architectures. *Polym Chem* 11:4068–4077
3. Chun C, Xiaojian M, Peilin C (2006) Kinetics of levulinic acid formation from glucose decomposition at high temperature. *Chin J Chem Eng* 14(5):708–712
4. Mikola M, Ahola J, Tanskanen J (2019) Production of levulinic acid from glucose in sulfolane/water mixtures. *Chem Eng Res Des* 148:291–297
5. Girisuta B, Janssen LPBM, Heeres HJ (2006) A kinetic study on the decomposition of 5-hydroxymethylfurfural into levulinic acid. *Green Chem* 8:701–709
6. Wang Y, Huang Y, Liu L et al (2020) Molecular oxygen-promoted synthesis of methyl levulinate from 5-hydroxymethylfurfural. *ACS Sustain Chem Eng* 8(38):14576–14583
7. Peng L, Lin L, Li H (2012) Extremely low sulfuric acid catalyst system for synthesis of methyl levulinate from glucose. *Ind Crops Prod* 40:136–144
8. Li H, Peng L, Lin L et al (2013) Synthesis, isolation and characterization of methyl levulinate from cellulose catalyzed by extremely low concentration acid. *J Energy Chem* 22:895–901
9. Peng L, Lin L, Li H et al (2011) Conversion of carbohydrates biomass into levulinate esters using heterogeneous catalysts. *Appl Energy* 88(12):4590–4596
10. Tominaga KI, Mori A, Fukushima Y et al (2011) Mixed-acid systems for the catalytic synthesis of methyl levulinate from cellulose. *Green Chem* 13:810–812
11. Nemoto K, Tominaga KI, Sato K (2014) Straightforward synthesis of levulinic acid ester from lignocellulosic biomass resources. *Chem Lett* 43(8):1327–1329
12. Zhou L, Zou H, Nan J et al (2014) Conversion of carbohydrate biomass to methyl levulinate with  $Al_2(SO_4)_3$  as a simple, cheap and efficient catalyst. *Catal Comm* 50:13–16
13. Saravanamurugan S, Riisager A (2013) Zeolite catalyzed transformation of carbohydrates to alkyl levulinates. *ChemCatChem* 5:1754–1757
14. Liu J, Yang BB, Wang XQ et al (2017) Glucose conversion to methyl levulinate catalyzed by metal ion-exchanged montmorillonites. *Appl Clay Sci* 141:118–124
15. Emeis CA (1993) Determination of integrated molar extinction coefficients for infrared absorption bands of pyridine adsorbed on solid acid catalysts. *J Catal* 141(2):347–354
16. Yang X, Yang J, Gao B et al (2019) Conversion of glucose to methyl levulinate over Sn-Al- $\beta$  zeolite: role of Sn and mesoporosity. *Catal Comm* 130:105783
17. Newsam JM, Treacy MMJ, Koetsier WT et al (1988) Structural characterization of zeolite beta. *Proc R Soc Lond A* 420(1859):375–405
18. Asbrink S, Waskowska A (1991) CuO: X-ray single-crystal structure determination at 196 K and room temperature. *J Phys* 3(42):8173
19. Davey WP (1925) Precision measurements of the lattice constants of twelve common metals. *Phys Rev* 25:753–761
20. Yamaguti T (1938) An investigation on oxidation of crystal surfaces with electron diffraction method, II. Copper single crystals. *Proc Phys-Math Soc Jpn* 20:230–241

**Publisher's Note** Springer Nature remains neutral with regard to jurisdictional claims in published maps and institutional affiliations.